journal of materials processing technology 206 (2008) 62–68

journal homepage: www.elsevier.com/locate/jmatprotec

Numerical simulation of metal flow and solidification in the multi-cavity casting moulds of automotive components

*A. Kermanpur**, *Sh. Mahmoudi*, *A. Hajipour*

Department of Materials Engineering, Isfahan University of Technology, Isfahan 84156-83111, Iran

ARTICLE INFO

Article history:
Received 1 November 2006
Received in revised form
17 November 2007
Accepted 2 December 2007

Keywords:
Numerical simulation
Casting
Solidification
Finite volume method
Automotive components

ABSTRACT

The metal flow and solidification behaviours in a multi-cavity casting mould of two automotive cast parts were simulated in three dimensions. The commercial code, FLOW-3D® was used because it can track the front of the molten metal by a volume-of-fluid (VOF) method and allows complicated parts to be modelled by the fractional area/volume obstacle representation (FAVOR) method. The grey iron automotive components including a brake disc and a flywheel were cast using an automatic sand casting production line. Solid models of the casting, the gating system and the ceramic filter were spatially discretised in a multi-block pattern. The surface roughness and the contact angle of the mould were taken into account in the model, based on the properties of the sand mould used. The turbulent flow was simulated using the two-equation k–ε turbulence model. The D'Arcy model was used to analyse the fluid flow throughout the ceramic filter designed in the gating system. The simulation model was validated against the experimental observations. The model was used to investigate the appropriateness of the multi-cavity mould design and its running system for each automotive component.

© 2007 Elsevier B.V. All rights reserved.

1. Introduction

Numerical simulation provides a powerful means of analysing various physical phenomena occurring during casting processes. It gives an insight into the details of fluid flow, heat transfer and solidification (Flemings, 1974; Campbell, 1991). Numerical solutions allow researchers to observe and quantify what is not usually visible or measurable during real casting processes. The goal of such simulations is to help shorten the design process and optimize casting parameters to reduce scrap, use less energy and, of course, make better castings. Simulation produces a tremendous amount of data that characterize the transient flow behaviour (*e.g.*, velocity, temperature), as well as the final quality of the casting (*e.g.*, porosity, grain structure). It takes good understanding of the actual casting process, and experience in numerical simulation, for a designer to be able to relate one to the other and derive useful conclusions from the results.

Most of the casting modelling codes can be divided into two categories: those using the finite difference (FD) approach for solving fluid flow equations, and those that employ the finite element (FE) method (Barkhudarov, 1998). The FE method uses body-fitted computational grids leading to more accurate representation of metal/mould interfaces than generally achievable by FD methods. However, generating good quality FE grids is still a challenging task and often takes significantly more time than the simulation itself. Solution accuracy degenerates in highly distorted grids and changes in geometry, even small ones, often require a completely new grid. The FD method offers ease of mesh generation due to the structured nature of the mesh, uses less storage to describe

* *Corresponding author*. Tel.: +98 311 3915738; fax: +98 311 3912752.
E-mail address: ahmad_k@cc.iut.ac.ir (A. Kermanpur).
0924-0136/$ – see front matter © 2007 Elsevier B.V. All rights reserved.
doi:10.1016/j.jmatprotec.2007.12.004

geometry and simplifies the implementation of the numerical algorithms. However, the conventional FD methods often require fine grids to describe complicated geometry to reduce errors associated with the 'stair-step' representation of curved boundaries. The latter introduces inaccuracies when computing liquid metal flow along the walls and heat fluxes normal to the walls.

In this work, the commercial, general purpose, computational fluid dynamics (CFD) code FLOW-3D®, was used to simulate the filling and solidification sequences of two automotive components, cast into the multi-cavity sand moulds (FLOW-3D, 2005). The process model developed was used to investigate the appropriateness of the running and feeding systems.

2. Model theory

The CFD code FLOW-3D® is based on a finite volume/finite difference approach. Two methodologies, fractional area/volume obstacle representation (FAVOR) and volume-of-fluid (VOF), constitute the core of the software. These methods differ from methods in most other codes but offer many advantages, and are summarised below (Barkhudarov and Hirt, 1993).

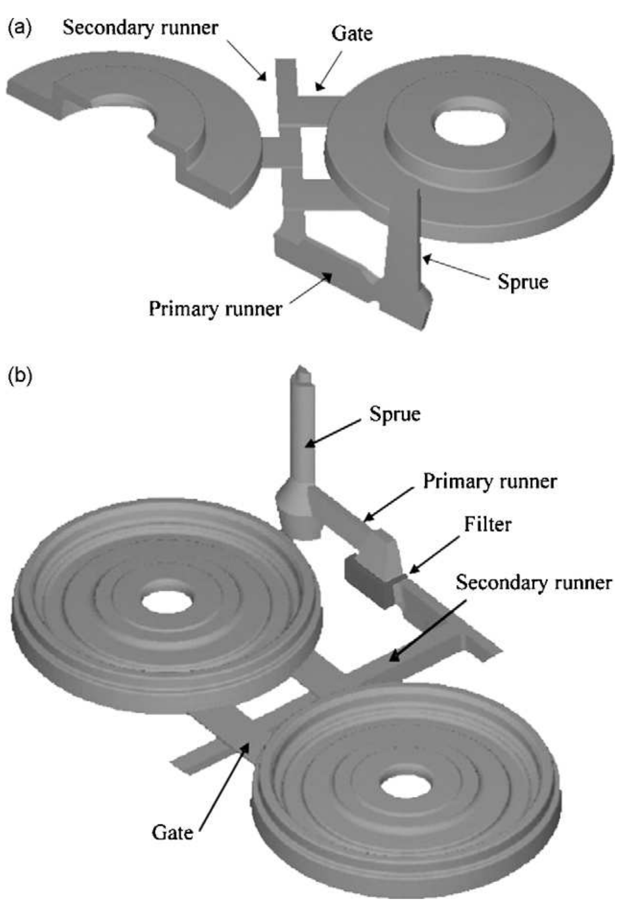

Fig. 1 – The solid models of the automotive components: (a) three-cavity brake disc and (b) four-cavity flywheel. Note that due to the symmetry, only half of the whole mould is modelled.

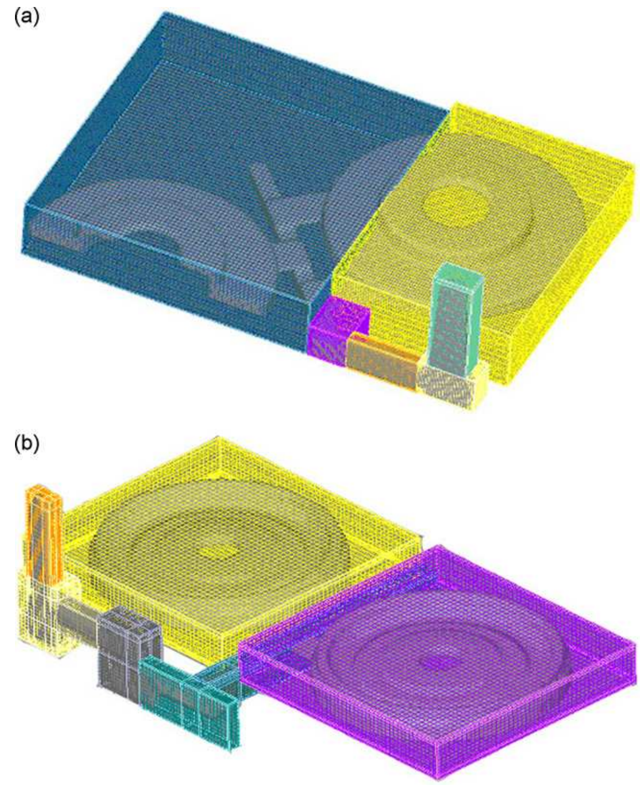

Fig. 2 – The multi-block meshes of the castings: (a) brake disc and (b) flywheel. Note that the mould mesh is not shown.

2.1. *Geometry representation*

An advancement of the conventional FD method is given by the FAVOR method. In this method rectangular grid cells can be partially blocked by obstacles (Hirt and Sicilian, 1985). The blockage is described by using fractional cell volumes and areas on cell sides. The FAVOR method improves the accuracy of the numerical solution near mould walls and allows for the use of coarser grids than in standard FD methods. Since the geometry representation is less mesh-dependent, the FAVOR method is also referred to as a 'free gridding' method.

For an incompressible, viscous fluid, the FAVOR equations take the form:

$$\nabla \cdot (\mathbf{Au}) = 0 \tag{1}$$

$$\frac{\partial \mathbf{u}}{\partial t} + \frac{1}{V}(\mathbf{Au} \cdot \nabla)\mathbf{u} = -\frac{1}{\rho}\nabla p + \frac{1}{\rho V}(\nabla \mathbf{A}) \cdot (\mu \nabla)\mathbf{u} + g \tag{2}$$

$$\frac{\partial H}{\partial t} + \frac{1}{V}(\mathbf{Au} \cdot \nabla)H = \frac{1}{\rho V}(\nabla \mathbf{A}) \cdot (k \nabla T) \tag{3}$$

where

$$H = \int C(T)\, \mathrm{d}T + L(1 - f_s) \tag{4}$$

In these equations A_i is the open area fraction associated with the flow in the ith direction, V the open volume fraction, ρ

Table 1 – Thermo-physical properties of the casting, mould and filter

Material	Property	Symbol	Value	Unit
Casting	Thermal conductivity of liquid	k_l	39.59	W/(m K)
	Thermal conductivity of solid	k_s	34.39	W/(m K)
	Specific heat of liquid	C_l	897	J/(kg K)
	Specific heat of solid	C_s	770	J/(kg K)
	Surface tension coefficient of liquid	σ	1.871	kg/s^2
	Kinematic viscosity	μ	0.0045	m^2/s
	Density of liquid	ρ_l	6856	kg/m^3
	Density of solid	ρ_s	7100	kg/m^3
	Latent heat	L	216	kJ/m^3
	Liquidus temperature	T_l	1504	K
	Solidus temperature	T_s	1420	K
Sand mould	Thermal conductivity	k_m	0.61	W/(m K)
	Volumetric specific heat	ρC	1700	kJ/(kg K)
Ceramic filter	Thermal conductivity	k_f	1.6	W/(m K)
	Volumetric specific heat	ρC	4660	kJ/(kg K)

density, p pressure, u_i the ith velocity component, μ the fluid viscosity coefficient, g gravity, H fluid enthalpy, T fluid temperature, f_s solid fraction, L latent heat, and C and k fluid-specific heat and thermal conductivity coefficient, respectively. For the mould, the energy equation has the form

$$\frac{\partial T_m}{\partial t} = \frac{1}{\rho C_m V_c}(\nabla \mathbf{A}_c) \cdot (k_m \nabla T_m) \qquad (5)$$

where the subscript m indicates a parameter related to the mould and the subscript c indicates quantities that are complements of the volume and area fractions. At the metal/mould interface, the heat flux, q, is calculated according to

$$q = h(T - T_m) \qquad (6)$$

where h is the heat transfer coefficient.

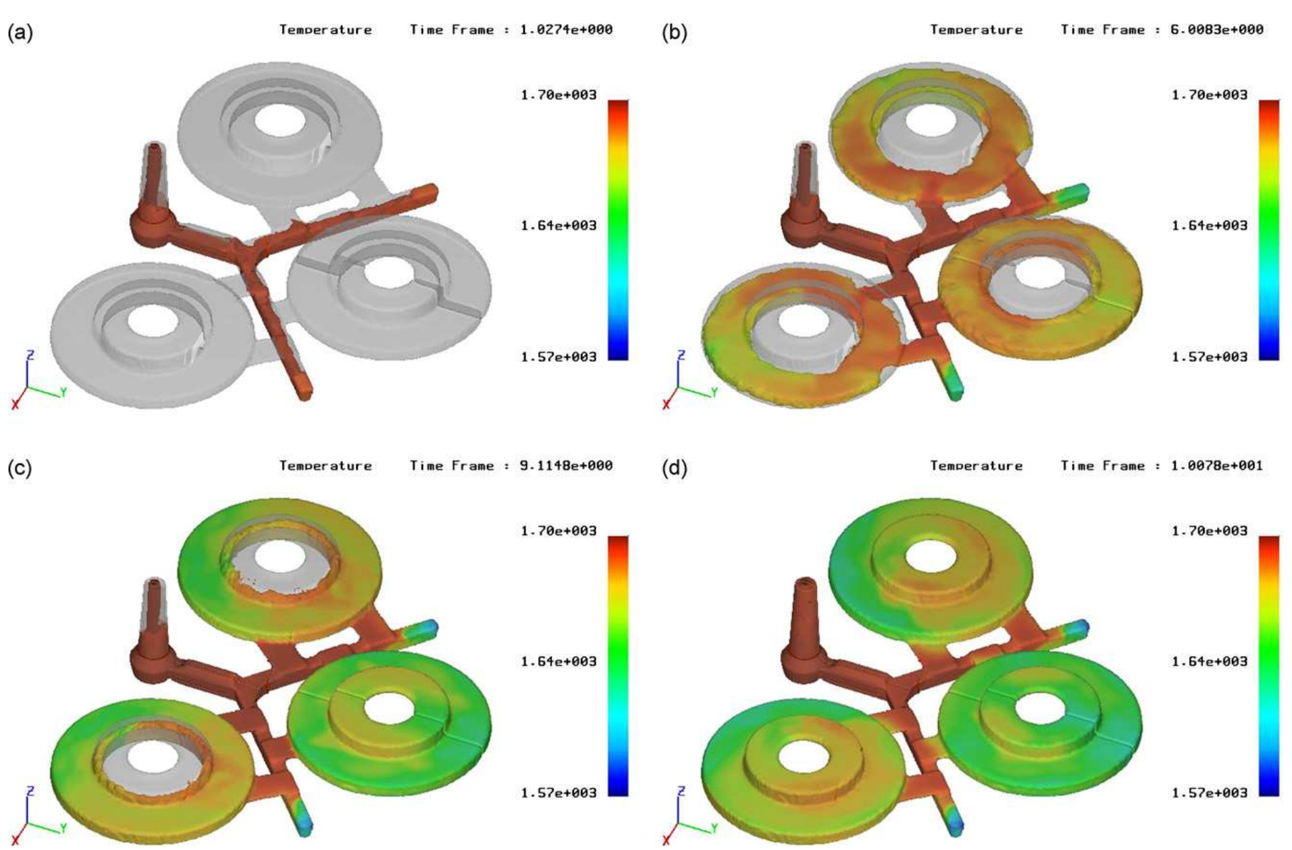

Fig. 3 – The filling sequences for the brake disc part cast in a three-cavity sand mould at different time: (a) 1.0 s, (b) 6.0 s, (c) 9.1 s, and (d) 10.1 s.

Table 2 – Experimental measurements of the filling and solidification times of the casing components

Components	Filling time (s)	Solidification time (s)
Brake disc	9.5	300
Flywheel	15	250

2.2. *Tracking the free surface*

Mould filling problems involve tracking free surfaces that are the boundaries between liquid metal and the surrounding air. The most commonly used method to describe free surfaces is the volume-of-fluid (VOF) method. The VOF method enables the tracking the transient-free surfaces with arbitrary topology and deformations (*e.g.*, fluid surface break-up and coalescence). The 'true' VOF method consists of three main components (Hirt and Nichols, 1981):

1. A fluid fraction function $F(t,\mathbf{r})$ which is equal to 1.0 in fluid regions, and equal to 0.0 in voids. Since fluid configurations may change with time, F is a function of time, t, as well as space, $\mathbf{r}$. Averaged over a computational control volume, the fluid fraction function has a fractional value in cells containing a free surface.
2. Zero shear stress and constant pressure boundary conditions are applied at free surfaces.
3. A special advection algorithm is used for tracking sharp-free surfaces.

The equation for the F function is

$$\frac{\partial F}{\partial t} + \frac{1}{V}\nabla \cdot (\mathbf{Au}F) = 0 \quad (7)$$

The boundary conditions at the free surface are zero normal and tangential stresses.

A free surface advection method must preserve the sharpness of the interface and have minimal free surface distortion. Generally, such advection algorithms are based on geometric reconstruction of the free surface using the values of F at grid nodes (Kothe and Rider, 1994). Sometimes a free surface is approximated by a density discontinuity between metal and air and flow equations are solved for both fluids. In that case it is difficult to enforce correct boundary conditions at the surface. This is because free surface pressure and velocities in the two-fluid approach are not set explicitly, but are computed by solving the flow equations and these flow equations are solved in terms of mixture variables. Since densities of liquid metal and air differ greatly (*e.g.*, by a factor of 7000 for steel), the mixture velocity may not always be an accurate measure of the relative motion of metal and air (Kothe and Rider, 1994).

3. Numerical simulation

Two automotive components including a brake disc and a flywheel were simulated in this work. The complete solid models of the parts were created in steriolithography (STL) format and imported to the software (Fig. 1). Due to the symmetry plane of the system, only half of each model was modelled. The multi-block meshes of the models are shown in Fig. 2. Thermo-physical properties of the cast iron parts, silica mould and ceramic filter, were derived from both literature and manufacturer's documents and are listed in Table 1. The surface roughness of the mould used was 25 μm and the contact angle was 180°. The initial velocity of the melt at 1703 K entering the sprue was 2.3 m/s based on the calculation of the total weight of the melt and the experimentally measured filling time. The heat transfer coefficient between the mould wall and the casting was assigned in the range of 600–1000 W/(m^2 K), according to the measurement of the total solidification time for each casting (Kermanpur et al., 2006a,b). The following assumptions were considered in the simulations (Barkhudarov and Hirt, 1993):

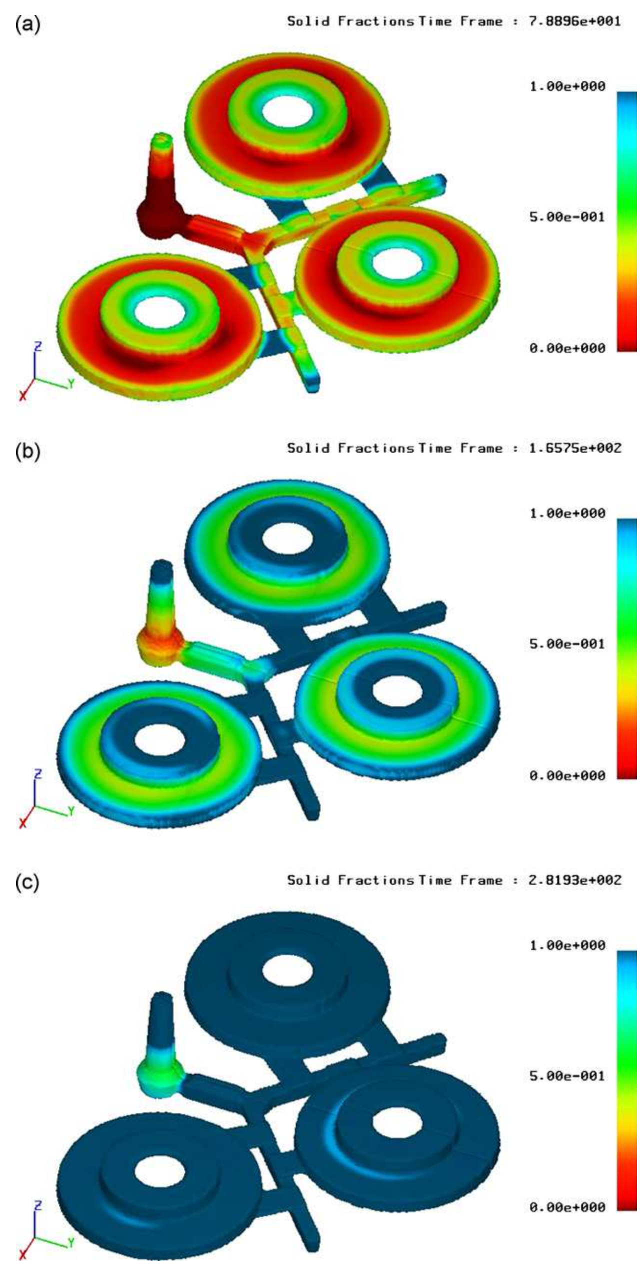

Fig. 4 – The solidification sequences for the brake disc part cast in a three-cavity sand mould at different time: (a) 78.9 s, (b) 165.8 s, and (c) 281.9 s.

1. Incompressible, Newtonian flow.
2. k–ε turbulence model.
3. Viscose heating.
4. D'Arcy model for the porous media.

Within a porous body, the flow of a fluid is resisted by viscous and geometric (tortuosity) effects. Flow losses in porous media can be modelled in a number of ways. Most common case is the D'Arcy-type flow in which the flow resistance is linearly proportional to velocity. Saturated flow in porous media is one such application. Another case might be the flow of air through a matrix of fibres as in a filter apparatus. For these cases, FLOW-3D® software has provisions for a volume fraction (or porosity)-dependent drag coefficient

$$K = aV_F^{-b} \tag{8}$$

where a and b are positive constants and V_F is the fractional volume open to flow. A zero value of b can be used when a constant drag coefficient is desired. The constants of the drag coefficient equation were assigned based on the data delivered by the filter manufacturer.

4. Experimental

In order to validate the simulation model, the filling time of each component was measured carefully by a precise stopwatch. The solidification time of the castings were determined by knocking out the moulds in different times after the pouring. Table 2 shows the filling and solidification times measured for the two castings. A Minolta/Land Cyclops 152 infrared pyrometer was used to measure the melt temperature just before pouring. All castings were cut transversely after cooling down to determine the location of any possible shrinkage.

5. Results

5.1. *Brake disc part*

The filling pattern of the three-cavity brake disc mould is shown in Fig. 3. The cast iron melt stream with a cross-sectional area less than that of the sprue is entered into the mould and fills up the primary runner followed by the secondary runner after about 1.0 s (Fig. 3a). The melt is then entered to the mould cavity through the second gate of the side-castings followed by the gates of the middle-casting, when the inclusion trap in the primary runner is completely filled. During the filling of the mould, it can be seen that the first gate of the side-castings are remained *partially filled* even until about 6.0 s during which the melt might suck the air through the mould (Fig. 3b). The mould filling process proceeds such that the middle-cavity is completely filled up sooner than the side-cavities (Fig. 3c and d). The simulated filling time is about 10.08 s, that is close to the experimentally measured one 9.5 s (see Table 1).

The solidification pattern of the brake disc component just after filling is shown in Fig. 4. The melt solidification is started around the gates such that all gates are completely solidified after about 80 s (Fig. 4a). The solidification follows from the low modulus sections like the internal and external edges towards the casting centre. The secondary runner is completely solidified after about 166 s (Fig. 4b). The side-castings

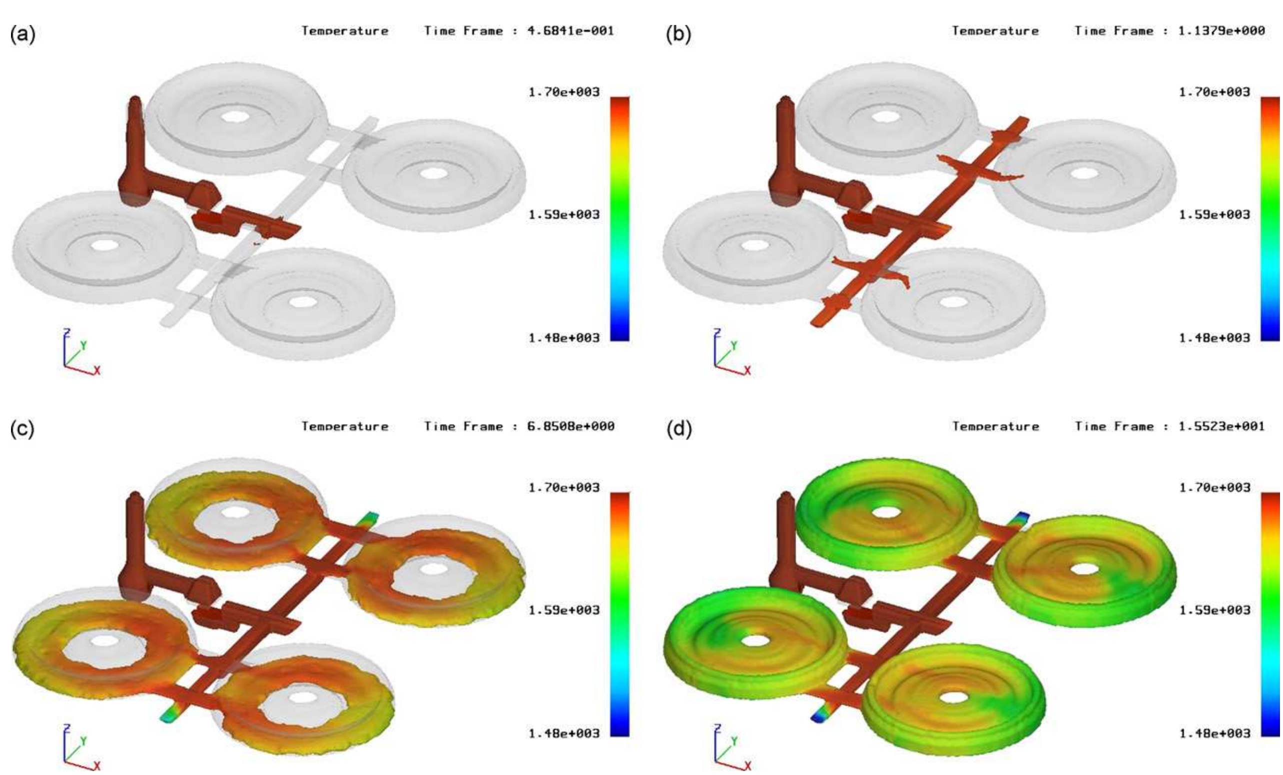

Fig. 5 – The filling sequences for the flywheel part cast in a four-cavity sand mould at different time: (a) 0.47 s, (b) 1.14 s, (c) 6.85 s, and (d) 15.52 s. Note that the filter is not shown in the figures.

and the middle-casting are finally solidified after 280 s and 300 s, respectively (Fig. 4c). The simulated solidification time 285 s is comparable to the measured one 300 s.

5.2. *Flywheel part*

The filling pattern of the four-cavity flywheel mould is shown in Fig. 5. The cast iron melt stream with a cross-sectional area less than that of the sprue is entered into the mould and after passing the filter, fills up the primary runner at 0.47 s (Fig. 5a). Note that the porous-media filter is shown as a transparent region. The secondary runner is then filled up, raising the melt level in the sprue. It is after about 1.14 s that the melt enters the gates and starts filling the cavities slowly (Fig. 5b). The simulated flow pattern shows that the first gate of all four castings in the mould remains *partially filled* even until about 6.9 s (Fig. 5c). The rest of the mould cavity is then filled up smoothly. As it is shown in Fig. 5d, the predicted filling time is about 15.5 s that is in agreement with the observations (Table 2). It is also seen that two cavities closer to the sprue are filled up sooner (about 0.2 s) than the others.

The solidification pattern of the flywheel cast parts just after filling is shown in Fig. 6. The melt solidification is started around the filter, top of the sprue and end of the secondary runner followed by the gates (Fig. 6a). After about 100 s, all gates as well as the filter chamber are completely solidified and the solidification of the cast part starts from the edges (Fig. 6b). The solidification of all castings takes place simultaneously about 220 s and the rest of the gating system solidifies approximately 50 s afterwards (Fig. 6c) showing a reasonable agreement with the measured values (Table 2). This solidification pattern shows a relatively suitable gating system design which leads to a reasonable casting efficiency.

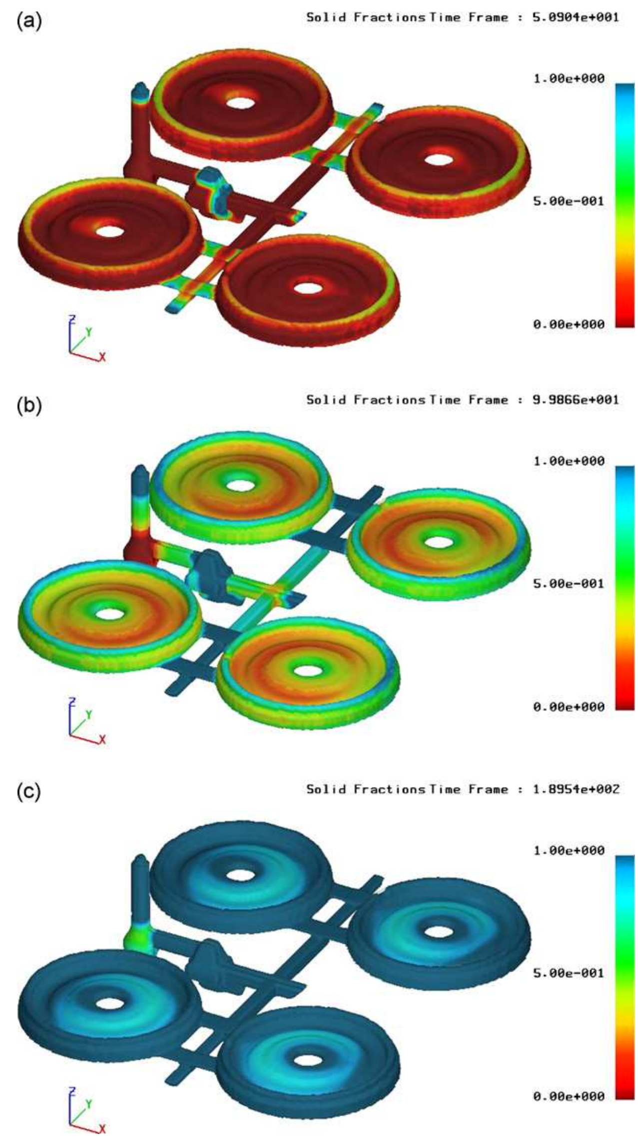

Fig. 6 – The solidification sequences for the flywheel part cast in a four-cavity sand mould at different time: (a) 50 s, (b) 100 s, and (c) 190 s.

6. Discussions

The verified model interestingly represented the correct location of the hot spots in the castings. Fig. 7 compares the simulated final location of the hot spots for the brake disc part with the micro-shrinkage that is experimentally observed, showing a reasonable agreement. It should be noted that due to the automatic moulding system being used, it was not possible to propose a suitable chilling system to avoid such micro-shrinkage. However, the simulation results showed that decreasing the superheat temperature is a practical parameter to significantly reduce the occurrence of such possible micro-shrinkage at this location (Kermanpur et al., 2006a,b).

The simulated results for metal flow pattern during the casting of both cast parts (see Figs. 3b and 5c) showed that the first gate of the gating system does not work properly, as it remains *partially filled* until about half of the mould filling period. This manner can cause air absorption by the melt, resulting in possible gas porosity in the final parts. It can be suggested that in order to decrease the chance for porosity formation in the castings, the cross-sectional area of the first gates of this gating system (*e.g.*, gate width), should be reduced (for example about one-third). This will not affect the flow pattern in the system. Another suggestion is to use a stepped-gate instead of using the gate with a uniform cross-sectional area. This suggestion worked out in practice (Kermanpur et al., 2006a,b).

Comparing the flow pattern for the flywheel with the brake disc shows that the use of filter in the gating system can also reduce turbulence of the melt, regardless of removing the inclusions. This can be a benefit for lowering probability of melt oxidation or sand washing as well.

The simulation results for both castings clearly demonstrated that all gates are properly solidified prior than the castings, making it possible for the melt to compensate its contraction during solidification by the expansion of graphite phase such that no riser is needed. Therefore, in terms of the solidification point of view, the cross-sectional area of the gates are designed satisfactory.

The solidification behaviour of the three-cavity brake disc mould showed a non-uniform manner for the side-castings compared to the middle-casting. On the other hand, the

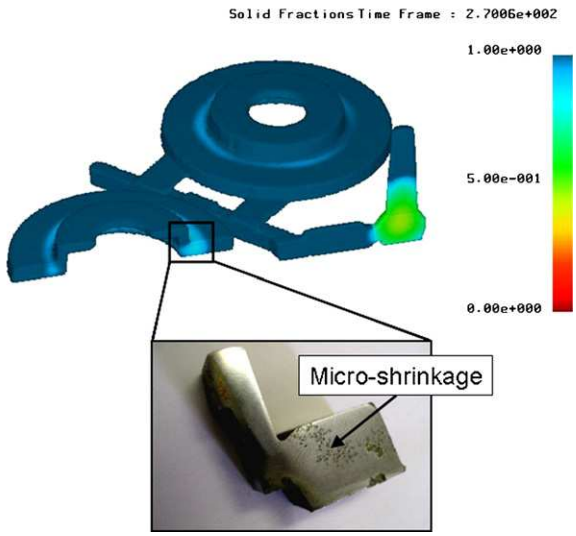

Fig. 7 – Comparison of predicted result for the hot spot with a micrograph of the cross section of the brake disc. The figure shows a good agreement between simulation and experiment.

four-cavity flywheel mould represented uniform solidification behaviour for all cast parts. It can be concluded that in order to establish a similar heat transfer and solidification conditions for all cast parts in each multi-cavity mould, it is necessary to consider symmetrical configuration. Therefore, a four-cavity mould is suggested for the brake disc part.

The present simulation model clearly shows the capability of analysing the fluid flow and solidification behaviours of the automatic casting process. This model is even capable of investigating the casting efficiency as well as testing the suitability of different gating system designs. The model is under development for tracking inclusion during the mould filling.

7. Conclusions

A 3D simulation model was developed to simulate the filling and the solidification behaviours of the automotive components, cast in an automatic sand casting production line. The verified model based on the experimental observations, showed that the four-cavity mould is more suitable than the three-cavity one, in getting a more uniform casting quality for all cast parts. The model also represented a different performance between the gates for each cast part, suggesting a smaller cross-sectional area for the first gate to reduce the risk of air absorption. The present simulation model is able to study the effects of several casting parameters including the melt superheat, pouring time (velocity), mould surface roughness, gating design, and the mould configuration on the quality and soundness of automotive cast parts.

Acknowledgments

The authors appreciate the collaboration of their colleagues at Isfahan University of Technology and Azarin Casting Industries of Isfahan, especially Mr. H. Morady.

REFERENCES

Barkhudarov, M.R., 1998. Advanced simulation of the flow and heat transfer in simultaneous engineering, Technical Report, Flow Science, Inc.

Barkhudarov, M.R., Hirt, C.W. Casting simulation: mold filling and solidification—benchmark calculations using FLOW-3D®, Technical Report, Flow Science, Inc., 1993.

Campbell, J., 1991. Castings. Butterworth Heinmann.

Flemings, M.C., 1974. Solidification Processing. McGraw-Hill Book Co., New York.

Flow Science, Inc., 2005. FLOW-3D® User's Manual, Version 8.2.

Hirt, C.W., Nichols, B.D., 1981. Volume of fluid (VOF) method for the dynamics of free boundaries. J. Comput. Phys. 39, 201–255.

Hirt, C.W., Sicilian, J.M., 1985. Proceedings of the 4th International Conference on Ship Hydrodynamics, Washington, DC, September 1985.

Kermanpur, A., Mahmoudi, Sh., Hajipour, A., 2006a. Numerical analysis of solidification of the cast iron automotive parts. In: Proceedings of the 8th Symposium of the Iron and Steel Society of Iran, Isfahan University of Technology, Februrary 28–March 1 2006, pp. 188–199.

Kermanpur, A., Hajipour, A., Mahmoudi, Sh., 2006b. Numerical simulation of fluid flow and solidification in the casting of an automotive flywheel part. In: Proceedings of the 14th Annual (International) Mechanical Engineering Conference (ISME2006), Isfahan University of Technology, Isfahan, Iran, May 2006.

Kothe, D.B., Rider, W.J. Comments on modelling interfacial flows with volume-of-fluid methods, Los Alamos National Laboratory Report LA-UR-94-3384, 1994.